Displacement Reactions in the Solid State

ROBERT A. RAPP, ANDRE EZIS, AND GREGORY J. YUREK

Simple displacement reactions in the solid state are considered with the purpose of predicting the morphologies and the reaction rates from a knowledge of pertinent thermodynamic and diffusion data. The theoretical predictions are substantiated by experimental observations for four reaction couples [Ni/Cu_2O, Co/Cu_2O, Fe/Cu_2O, and Fe/NiO] reacted at 1000°C. Displacement reactions are classified according to the product morphology; layered and aggregate arrangements of the product phases were observed, with two modifications (lamellar and interwoven) occurring within the aggregate morphological class. Parabolic kinetics for the growth of the product phases are observed for each couple. The magnitudes of the parabolic rate constants for the couples which exhibit the layered arrangement are comparable with calculated values. A technique for controlling the product morphology is discussed, and a process for producing porous metal or oxide screens is introduced.

IN metal-matrix composites and other high-temperature materials, the occurrence of displacement reactions between metal matrices and compound fibers, particles, or precipitates is an important consideration. The purpose of the present investigation is the prediction (or rationalization) of morphologies and kinetics for simple displacement reactions from a knowledge of the thermodynamic and kinetic properties of the phases involved.

THEORETICAL ANALYSIS

Consider the following simple displacement reaction involving the metals M and Me, and their lowest oxides M_xO and $Me_\nu O$

$$\nu Me + M_xO \rightarrow Me_\nu O + xM \qquad [I]$$

Negligible mutual solubility is assumed for the phases M and $Me_\nu O$, Me and M_xO, M_xO and $Me_\nu O$, and Me and M. It is assumed that no other binary compounds and no ternary compounds are formed by the reaction. Finally, the phases involved are assumed to exhibit predominant electronic conduction, and except when otherwise mentioned, the product oxide is assumed to exhibit predominant cation diffusion. Although only oxides are considered herein, the analysis should also be applicable (where the assumptions are valid) to nitrides, carbides, silicides, borides, sulfides, and other compounds.

The Gibbs free energy change per mole of oxygen for reaction [I] is

$$\Delta G_I = \Delta G^\circ_{Me_\nu O} - \Delta G^\circ_{M_xO} \qquad [1]$$

if metal saturated with respect to its lowest oxide and oxide saturated with respect to the metal are chosen as the standard states for the phases. In terms of the oxygen activities for metal/oxide coexistence, ΔG_I can also be expressed as

$$\Delta G_I = \frac{RT}{2} \ln \frac{P_{O_2}(Me/Me_\nu O)}{P_{O_2}(M/M_xO)} \qquad [2]$$

ROBERT A. RAPP and GREGORY J. YUREK are Professor and Graduate Student, respectively, Department of Metallurgical Engineering, The Ohio State University, Columbus, Ohio 43210. ANDRE EZIS is Research Engineer, The Ford Motor Company, Dearborne, Mich.

Manuscript submitted September 12, 1972.

A spontaneous reaction should result from the contact at high temperatures of phase combinations such as Fe/NiO, Fe/Cu_2O, Co/Cu_2O, Ni/Cu_2O, and so forth. While the magnitudes of the Gibbs free energies of reaction for the indicated pairs differ considerably, large differences also exist in the cation diffusivities in the product oxides and in the oxygen permeabilities in the product metals.

Wagner[1] has considered the morphological and kinetic aspects of displacement reactions in the solid state. He pointed out that, in principle, the reaction product phases might form either a) adjacent to one another (to yield an *aggregate* arrangement as shown schematically in Fig. 1(*a*)) or (*b*) behind one another (to yield a *layered* arrangement as shown schematically in Fig. 1(*b*)). Wagner explained that significant plastic deformation must occur in the product phases for the aggregate arrangement of Fig. 1(*a*), because of the large volume changes involved in the reaction. Furthermore, the actual microstructure for the reaction zone in the aggregate arrangement should be a disordered conglomerate of the product phases in contrast to the schematic illustration of Fig. 1(*a*).

A criterion to predict the type of product morphology for a given reaction couple has not been considered previously. The actual product morphologies resulting from displacement reactions and their relation to the limiting aggregate and layered arrangements receive further experimental investigation and rationalization in this study. First, however, a criterion to predict the arrangement of the product phases will be presented.

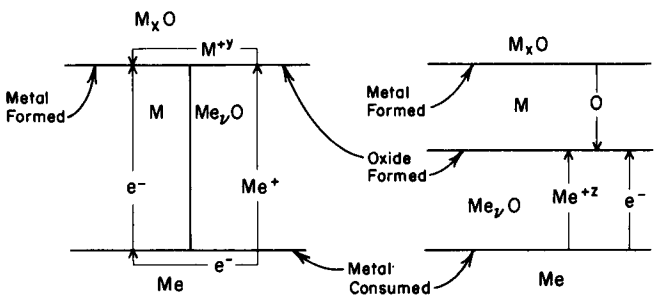

a. Aggregate Arrangement *b. Layered Arrangement*

Fig. 1—Schematic illustrations of possible product morphologies for displacement reactions in the solid state (after C. Wagner[1]).

In a paper concerned with the description of morphologies resulting from the diffusion-controlled oxidation of alloys, Wagner[2] has established a criterion for the stability of a flat growth interface. This criterion is adapted here for the case of displacement reactions. In Fig. 2 the $M/Me_\nu O$ interface in a layered arrangement of the products is tentatively assumed to be wavy. It is assumed that local equilibrium exists at the reaction interfaces and that the reaction rate is limited only by diffusion of the reacting species in the product phases.

If the growth of the $Me_\nu O$ phase is limited by cation diffusion within the $Me_\nu O$ phase, then the flux of cations arriving at position I exceeds that at position II. With a higher growth rate at position I, a flat $M/Me_\nu O$ interface would be stable and the interface would become flat. Alternatively, if the growth of the $Me_\nu O$ phase were limited by a step in advance of the $M/Me_\nu O$ interface (the relatively difficult transport of oxygen through the metal as considered here, or in general, a slow reaction at the M/M_xO interface), then the flux of oxygen arriving at position II would exceed that at position I. Under these conditions, the more rapid growth at position II would lead to a clefted or serrated interface and a flat growth interface for $Me_\nu O$ would be unstable; a two-phase product zone (*i.e.*, the aggregate morphology) would result. Although capillarity effects could stabilize a slightly wavy interface in the latter case, the driving forces are so large in the present situation that such effects are negligible.

For any couple having the layered morphology, the phase M would grow by the dissociation of M_xO at the M/M_xO interface with the dissolution and transport of oxygen atoms in the metal M. If the dissociation step maintains local equilibrium at the M/M_xO interface then the growth of phase M is necessarily controlled by the transport of oxygen through M, and thus, a flat M/M_xO interface should always be stable. For this reason, the occurrence of the layered or the aggregate arrangement should be decided solely by the stability of either a flat or a serrated $M/Me_\nu O$ interface, respectively. The type of $M/Me_\nu O$ interface which forms is determined by the rate-controlling step in the growth of the $Me_\nu O$ phase, as described above. The meaning of the "rate-controlling step" in a sequence of steps which all occur at the same net rate has been discussed recently.[3]

If the product oxide phase, $Me_\nu O$, should exhibit predominant anion diffusion (contrary to an initial assumption) then the growth of the $Me_\nu O$ phase would necessarily occur at the $Me/Me_\nu O$ interface. The growth of the $Me_\nu O$ product layer would be controlled by the diffusion of anions through this phase, or by the diffusion of oxygen through the M phase, so that the layered morphology of Fig. 1(*b*) would always be expected if the product oxide should exhibit predominant anion diffusion. Experiments verifying this prediction will be presented in a later publication.

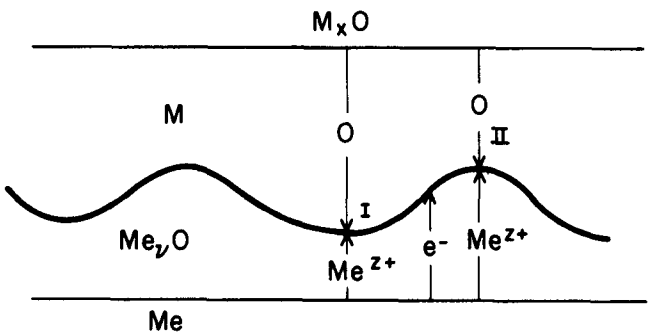

Fig. 2—Schematic illustration of a displacement reaction with a layered morphology and a tentatively assumed uneven interface.

EVALUATION OF THEORY

In order to examine quantitatively the proposed selection criterion, consider the reaction between nickel and Cu_2O at 1000°C and assume tentatively that the layered morphology of Fig. 1(*b*) would result. As a limiting case, assume that essentially the entire free energy change occurs across the NiO layer, and that only a very small gradient in oxygen activity exists across the copper. Actually, some gradient must exist across the copper because the flux of oxygen, j_O(Cu), through the copper is equivalent to the flux of nickel, j_{Ni}(NiO), through NiO oxide according to the stoichiometric requirements for the reaction $Ni + Cu_2O \rightarrow NiO + 2Cu$. With local equilibrium at the Cu/Cu_2O interface, the rate of growth of the NiO layer should equal that for the diffusion-controlled oxidation of pure nickel in a gas of oxygen activity corresponding to the coexistence of copper and Cu_2O. The rate of reaction should then be described by Wagner's[4] parabolic oxidation rate theory, whereby

$$\frac{d\tilde{n}}{dt} = \frac{1}{\xi}\left\{\frac{c_{eq}}{2}\int_{P'_{O_2}}^{P''_{O_2}} \frac{z_{cat}}{|z_{an}|}(D^*_{cat})d\ \ln P_{O_2}\right\} \qquad [3]$$

where the term in brackets is k_γ, Wagner's rational rate constant, and $d\tilde{n}/dt$ is the reaction rate with units of equivalents/cm^2-s. In Eq. [3], ξ is the thickness of the product layer, c_{eq} is the number of equivalents of product oxide/cm^3, D^*_{cat} is the self-diffusion coefficient for cations, z_{cat} and z_{an} are the valences of the ions, and P'_{O_2} and P''_{O_2} are the oxygen activities at the metal/oxide and oxide/gas interfaces, respectively.

Displacement reactions in the solid state are most readily studied by the microscopic measurement of the thickness of the reaction product layer. Eq. [3] can be converted by using Eq. [4]:

$$\frac{d\xi}{dt} = \frac{d\tilde{n}}{dt}\cdot\frac{1}{c_{eq}} \qquad [4]$$

With the substitution of Eq. [4] into Eq. [3] and integration,

$$\xi^2 = 2\left\{\frac{1}{2}\int_{P'_{O_2}}^{P''_{O_2}} \frac{z_{cat}}{|z_{an}|}(D^*_{cat})d\ \ln P_{O_2}\right\}t$$

$$= 2k_p(NiO)t \qquad [5]$$

where the term in brackets is the parabolic rate constant, k_p(NiO), for the diffusion-controlled growth of the NiO layer. At 1000°C, P'_{O_2} for Ni-NiO coexistence[5] equals $10^{-10.3}$ atm, P''_{O_2} for Cu-Cu_2O coexistence[5] equals $10^{-6.24}$ atm, and z_{Ni}/z_O equals unity. Although the thermodynamic data are well established, selection of an expression for D^*_{Ni}(NiO) and its P_{O_2}-dependence is

fraught with uncertainties, which will be discussed later in the Results and Discussion section. If we tentatively accept the recent work of Crow:[6]

$$D^{*}_{Ni}(NiO) = 8.9 \times 10^{-3}\, P_{O_2}^{1/6} \exp(-54{,}700/RT) \quad [6]$$

For 1000°C, Crow's expression is in good agreement with that of Lindner and Akerstrom,[7] but is a factor of five lower than the single crystal results of Choi and Moore,[8] and as much as an order of magnitude lower than values obtained from measurements of the chemical diffusion coefficient.[9,10] Substitution of Eq. [6] into Eq. [5] and integration gives

$$k_p(NiO) = 7.7 \times 10^{-13}\ cm^2/s \quad [7]$$

which should describe the parabolic growth of a flat, compact NiO layer in the Ni/Cu_2O displacement reaction, if Eq. [6] is appropriate.

Now, consider a second limiting case, namely that the entire Gibbs free energy change occurs across the copper layer for a layered morphology such as in Fig. 1(*b*). This limiting case should represent an unrealistic condition because it is equivalent to assuming that the reaction kinetics are controlled by the transport of oxygen through the copper, and under this condition, the aggregate arrangement of Fig. 1(*a*) would be expected to predominate. For each mole of oxygen transported through the copper, two moles of copper would be added to the copper layer. The use of Sieverts' law, a linear oxygen concentration profile across the copper layer, and a concentration-independent diffusion coefficient are justified. Then

$$\frac{dX}{dt} = 2V_{Cu} j_O(Cu) = 2V_{Cu} D_O^{Cu} \frac{\Delta c_O}{X} \quad [8]$$

where V_{Cu} is the molar volume of Cu, $j_O(Cu)$ is the flux of oxygen atoms through the copper layer (mole/cm^2-s), X is the thickness of the copper layer, D_O^{Cu} is the diffusivity of oxygen in copper, and Δc_O is the difference in oxygen content (mole/cm^3) across the copper layer. From Sieverts' law,

$$c_O = k_S P_{O_2}^{1/2} = \frac{N_O^{Cu}}{V_{Cu}} \quad [9]$$

where k_S is the Sieverts'-law constant and N_O^{Cu} is the atom fraction of dissolved oxygen in copper. At Cu-Cu_2O coexistence,[11] N_O^{Cu} equals 1.7×10^{-4} at 1000°C, and with V_{Cu} equal to 7.13 cm^3/mole,

$$k_S = 3.15 \times 10^{-2}\ \frac{\text{mole oxygen}}{cm^3\text{-atm}^{1/2}} \quad [10]$$

With the substitution of Eqs. [9] and [10] into Eq. [8] and integration

$$X^2 = 2[2V_{Cu} D_O^{Cu} k_S (P''^{1/2}_{O_2} - P'^{1/2}_{O_2})]t = 2k_p(Cu)t \quad [11]$$

where the term in brackets represents $k_p(Cu)$, the parabolic rate constant for the growth of the copper layer if oxygen transport through the copper were rate controlling. With D_O^{Cu} equal to 3.0×10^{-5} cm^2/s at 1000°C,[11] evaluation of Eq. [11] gives

$$k_p(Cu) = 1.0 \times 10^{-8}\ cm^2/s \quad [12]$$

Because of the difference in molar volumes, $k_p(NiO)$ and $k_p(Cu)$ cannot be compared directly; however, multiplication of k_p by c_{eq} for each phase yields comparable rational rate constants, k_r, which are defined by the expressions

$$\tilde{n}^2(NiO) = \xi^2(NiO) c_{eq}^2(NiO) = 2c_{eq}(NiO) k_r(NiO) t \quad [13a]$$

and

$$\tilde{n}^2(Cu) = X^2(Cu) c_{eq}^2(Cu) = 2c_{eq}(Cu) k_r(Cu) t \quad [13b]$$

where $\tilde{n}$ is the extent of the reaction and has units of equivalents/cm^2. At 1000°C, from Eqs. [7] and [13a] with $V_{NiO} = 11$ cm^3/mole

$$k_r(NiO) = c_{eq}(NiO) k_p(NiO) = 1.4 \times 10^{-13}\ \frac{\text{equiv}}{\text{cm-s}} \quad [14a]$$

and from Eqs. [12] and [13b],

$$k_r(Cu) = c_{eq}(Cu) k_p(Cu) = 1.4 \times 10^{-9}\ \frac{\text{equiv}}{\text{cm-s}} \quad [14b]$$

For the chosen example of the Ni/Cu_2O displacement reaction, the copper layer formed would be able to transport oxygen at a rate which is 10,000 times faster than cations could be transported through NiO for the same free energy change. In accord with the previous discussion, the tentatively postulated layered arrangement of product phases would be expected.

In general, the calculated values of k_r for the parabolic growth of the individual metal and oxide product layers in a presupposed layered arrangement should indicate whether the layered or the aggregate morphology is stable, such that

a) for $k_r(M) > k_r(Me_\nu O)$, the layered arrangement is stable

b) for $k_r(M) < k_r(Me_\nu O)$, the aggregate arrangement is stable.

When the resulting calculation indicates that the value of $k_r(M)$ is an order of magnitude or more greater than $k_r(Me_\nu O)$, then the product oxide of the layered arrangement should grow according to the calculated value of $k_p(Me_\nu O)$. Thus, the calculated value of $k_p(Me_\nu O)$ also serves to predict the kinetics of a displacement reaction which results in the layered arrangement. Because the growth of the product metal for a layered morphology is limited by the growth of the product oxide, the growth of this layer should be described by the rate constant

$$k'_p(M) = [c_{eq}(Me_\nu O)/c_{eq}(M)]^2 k_p(Me_\nu O) \quad [15]$$

For a Ni/Cu_2O couple at 1000°C, Eq. [15] gives

$$k'_p(Cu) = 1.3 \times 10^{-12}\ cm^2/s \quad [16]$$

With the use of the theoretical selection criterion which was just evaluated for the Ni/Cu_2O couple, let us now examine the Fe/Cu_2O and Fe/NiO couples at 1000°C. For each of these couples, a complication arises in that the phase Fe_3O_4 as well as wustite, "FeO", might be formed. From thermodynamic data[5] at 1000°C, $P_{O_2}(Fe/Fe_xO) = 10^{-14.85}$ atm and $P_{O_2}(Fe_yO/Fe_3O_4) = 10^{-12.74}$ atm. If we tentatively assume that the layered morphology would be formed, implying rate control by diffusion in the oxide, the layer sequences could appear as follows: $Fe|FeO|Fe_3O_4|Cu|Cu_2O$ or $Fe|FeO|Fe_3O_4|Ni|NiO$. However, in the oxidation of iron at high P_{O_2} only relatively thin layers of the higher oxides Fe_3O_4 and Fe_2O_3 are formed and the oxidation rate is not increased significantly with an increase in P_{O_2} above

that corresponding to Fe_yO/Fe_3O_4 coexistence. Then, in the calculation of k_p(FeO) by Eq. [5] for the Fe/Cu_2O and Fe/NiO couples, P''_{O_2} can be set equal to $P_{O_2}(Fe_yO/Fe_3O_4) = 10^{-12.74}$ atm. To calculate k_p(Cu) and k_p(Ni) according to Eq. [11], the value of P'_{O_2} can be set equal to $P_{O_2}(Fe_yO/Fe_3O_4)$. This choice is not critical because the term $P'^{1/2}_{O_2}$ is essentially negligible relative to $P''^{1/2}_{O_2}$ in Eq. [11] for these couples.

The dependence of the composition of wustite on P_{O_2} at 1000°C was determined by employing the results of Vallet and Raccah:[12]

$$(O/Fe) = 1.94P^{0.018}_{O_2} = (z_{cat}/z_{an}) \quad [17]$$

By combining the diffusion data of Himmel, *et al.*[13] and of Hembree and Wagner[14] with the composition data of Vallet and Raccah,[12] the following tracer-diffusion coefficient for cations in wustite was obtained as a function of composition at 1000°C:

$$D^T_{Fe}(FeO) = 5.89 \times 10^{-5} P^{0.21}_{O_2} \quad [18]$$

With the assumption that only a negligible correlation effect exists for the diffusion of radioactive iron ions in wustite,[15] the self-diffusion coefficient, D^*_{Fe} (FeO), may be taken as equal to the tracer-diffusion coefficient of Eq. [18]. Then,

$$k_p(FeO) = \frac{1}{2}\int_{10^{-14.85}}^{10^{-12.74}} (1.14 \times 10^{-4} P^{-0.77}_{O_2}) dP_{O_2}$$

$$= 2.1 \times 10^{-7} \text{ cm}^2/\text{s} \quad [19]$$

The calculation of k_p(Cu) from Eq. [11] using the previously mentioned data yields

$$k_p(Cu) = 1.0 \times 10^{-8} \text{ cm}^2/\text{s} \quad [20]$$

If k_p(FeO) and k_p(Cu) for the Fe/Cu_2O couple are converted to k_r values for comparison ($V_{Fe_{0.89}O}$ = 11.5 cm^3/mole)

$$k_r(FeO) = 3.7 \times 10^{-8} \text{ equiv/cm-s} \quad [21a]$$

and

$$k_r(Cu) = 1.4 \times 10^{-9} \text{ equiv/cm-s} \quad [21b]$$

Because k_r(FeO) is greater than k_r(Cu), the presupposed layered arrangement should be unstable, and the aggregate morphology would be expected for Fe/Cu_2O couples.

For the reaction of a Fe/NiO couple at 1000°C, the values of k_p(FeO) from Eq. [19] and k_r(FeO) from Eq. [21a] should again be valid, because the highest "effective" P_{O_2} possible for FeO again corresponds to $P_{O_2}(Fe_yO/Fe_3O_4)$. To calculate k_p(Ni), the solubility of oxygen in nickel is chosen as 350 ppm ($N^{Ni}_O = 3.5 \times 10^{-4}$) from Alcock and Brown.[16] The diffusivity of oxygen in nickel is selected from a recent study by Kerr and Rapp[17] as 6.0×10^{-8} cm^2/s at 1000°C.

In the evaluation of Eq. [11], P'_{O_2} [equal to $P_{O_2}(Fe_yO/Fe_3O_4)$] is small relative to P''_{O_2} [equal to P_{O_2} (Ni/NiO)]. Therefore, with one mole of nickel formed per mole of oxygen transported, Eq. [11] may be written as

$$X^2 = 2N^{Ni}_O D^{Ni}_O t \quad [22]$$

so that $N^{Ni}_O D^{Ni}_O$ equals k_p(Ni). Then for the Fe/NiO couple at 1000°C,

$$k_p(Ni) = 2 \times 10^{-11} \text{ cm}^2/\text{s} \quad [23]$$

and corresponding to Eq. [14b], with V_{Ni} equal to 6.6 cm^3/mole

$$k_r(Ni) = 6.1 \times 10^{-12} \text{ equiv/cm-s} \quad [24]$$

Comparison of k_r(Ni) from Eq. [24] with k_r(FeO) from Eq. [21a] indicates that the aggregate morphology, and not the tentatively postulated layered morphology, should be stable.

Tracer-diffusion data are available for CoO, so that calculations and predictions can be made for the Co/Cu_2O couple. In this couple, CoO and copper are assumed to be the resulting product phases. From the data of Carter and Richardson,[18] which agree with those of Crow,[6] at 1000°C

$$D^T_{Co}(CoO) = 2.6 \times 10^{-9} P^{0.35}_{O_2} \text{ cm}^2/\text{s} \quad [25]$$

With the assumption that $D^*_{Co}(CoO) \sim D^T_{Co}(CoO)$, substitution of Eq. [25] into Eq. [5] and integration between $P''_{O_2}(Cu/Cu_2O)$ and $P'_{O_2}(Co/CoO) = 10^{-11.9}$ atm from Ref. [5] gives

$$k_p(CoO) = 3.1 \times 10^{-11} \text{ cm}^2/\text{s} \quad [26]$$

or, with V_{CoO} = 11.6 cm^3/mole,

$$k_r(CoO) = 5.3 \times 10^{-12} \text{equiv/cm-s} \quad [27]$$

for the Co/Cu_2O couple. Evaluation of Eq. [11] gives

$$k_p(Cu) = 1.0 \times 10^{-8} \text{ cm}^2/\text{s} \quad [28]$$

or

$$k_r(Cu) = 1.4 \times 10^{-9} \text{ equiv/cm-s} \quad [29]$$

The comparison of k_r(CoO) and k_r(Cu) for the Co/Cu_2O couple at 1000°C indicates that the layered morphology should result with the kinetics described by Eq. [26] and

$$k'_p(Cu) = 4.7 \times 10^{-11} \text{ cm}^2/\text{s} \quad [30]$$

The calculated values for k_r and k'_p (for layered morphologies) and the predicted morphological modes have been listed in Table I for the four reactive couples which have been examined.

EXPERIMENTAL PROCEDURE

Solid cylindrical specimens 1 cm in diameter and 0.06 cm thick of Fe (purity >99.9 pct Fe), Ni (purity >99.9 pct Ni), and Co (purity >99.9 pct Co) were used for the reactions. Similarly-sized powder compacts of reagent-grade NiO and CoO were made. Prior to reaction, the powder compacts were sintered at 1075°C for 48 h. Solid Cu_2O slabs were made by the complete reaction of 99.999+ pct Cu slabs in an Ar-1 pct O_2 gas at 1025°C such that CuO was not stable and did not form. After oxidation, the Cu_2O specimens were sliced with a diamond saw and lapped. For some experiments, slices from a NiO single crystal (purity >99.9 pct NiO) were used.

After the faces of the specimens for a given reactive couple had been ground and polished to produce flat, parallel and smooth faces, the specimens were assembled into a spring-loaded holding device which would position the specimens in the center of the hot zone of

a resistance-heated tube furnace. This "cell holder" has been previously described.[5]

The specimens in the cell holder were placed into the heated furnace and reached the experimental temperature of 1000°C within 20 min. A stream of purified argon passed over the couple. To minimize chemical interactions between this gas and the couple, a combustion boat filled with coexistent *Me* and $Me_\nu O$ (with the lower P_{O_2} of the components in the couple) was placed immediately upstream from the couple. After the short transient upon heatup, the temperature of the cell was maintained at 1000° ± 1°C with the help of a thermocouple modulator which was recently described by Burt.[16] To conclude an experimental run, the cell holder was withdrawn from the furnace over a period of 3 to 5 min.

The reacted couples were mounted, sectioned, polished, and examined in a metallograph. The thickness of the product layers were measured using a scribed ocular lens which was calibrated against a stage micrometer. For couples with varying product layer thickness (resulting from imperfect initial contact of the specimens) the largest measurements from two cross-sectional cuts were accepted.

Some specimens were further examined in a scanning electron microscope (Materials Analysis Company, Model 700). When possible, X-ray diffraction was used to identify the product phases.

RESULTS AND DISCUSSION

Ni/Cu_2O Reaction: A photomicrograph of the layered product morphology formed upon the reaction of nickel and Cu_2O at 1000°C is shown in Fig. 3. The layered morphology is expected from the evaluation of the selection criterion according to Eqs. [14a] and [14b]. As is often encountered in the gaseous oxidation of nickel to form NiO, the oxide product consists of a compact external scale and a fine-grained inner scale. Upon cooling, a crack formed to split the NiO scale.

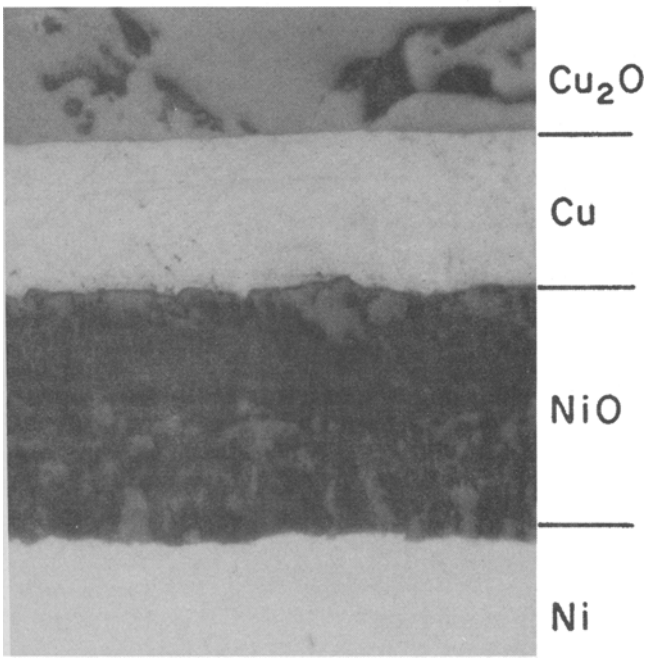

Fig. 3—Layered product morphology for the Ni/Cu_2O displacement reaction after 72 h at 1000°C. Magnification 700 times.

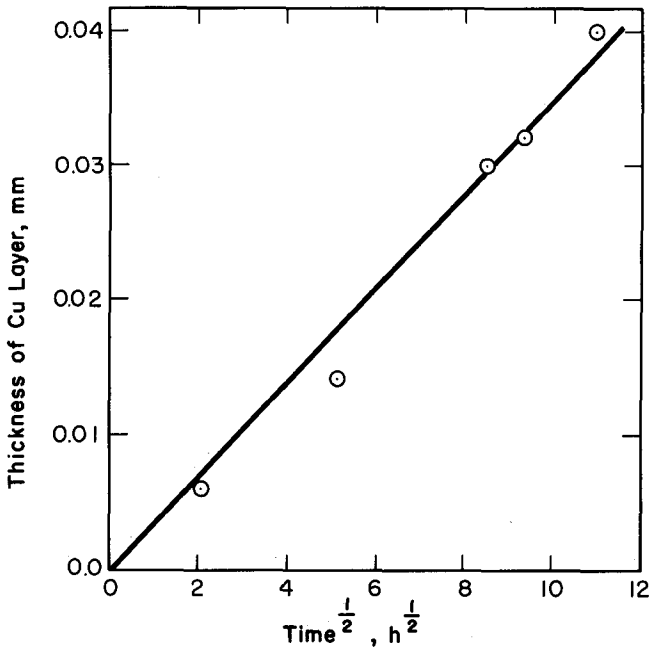

Fig. 4—Time dependence of the thickness of the product copper layer in the layered morphology for the Ni/Cu_2O displacement reaction at 1000°C.

The uniform thickness of the product copper layer is quite suitable for microscopic measurement; a plot of the thickness of the copper layer vs the square root of the reaction time for five experimental runs is shown in Fig. 4. The linearity of this plot indicates that the rate of the displacement reaction is indeed controlled by diffusion as opposed to a rate-limiting step at an interface. The value of the rate constant k'_p(Cu) derived from the slope of Fig. 4 is entered into Table I for comparison with the predicted rate constant. The observed reaction rate is a factor of about thirteen greater than the predicted rate. This disagreement is not considered serious as it probably arises from the following three sources: 1) the uncertainty in the value for D^*_{Ni}(NiO) used for the calculation, 2) the presence of impurity dopant ions in the NiO, and 3) the occurrence of the two-layered NiO scale, which probably contained considerable porosity and which is in contrast to Wagner's model for diffusion-controlled oxide growth. The product morphology of the Ni/Cu_2O reaction couple seems to represent the ideal layered arrangement of Fig. 1(*b*).

Co/Cu_2O Reaction: The CoO and Cu product layers resulting from the reaction of cobalt and Cu_2O at 1000°C are shown in Fig. 5. The observed layered morphology agrees with the expectations from the comparison of Eqs. [27] and [29].

As is also observed in the gaseous oxidation of cobalt, the inner, fine-grained portion of the two-layered CoO scale is less pronounced than that for NiO formed on nickel. The Co/Cu_2O couples also exhibited parabolic reaction rates as indicated in Fig. 6. The value for k'_p(Cu) from the slope of Fig. 6 is listed in Table I; it is about a factor of three higher than the calculated value. This better agreement is obtained probably because the higher native cation vacancy concentration of CoO leads to a lower sensitivity of CoO to aliovalent

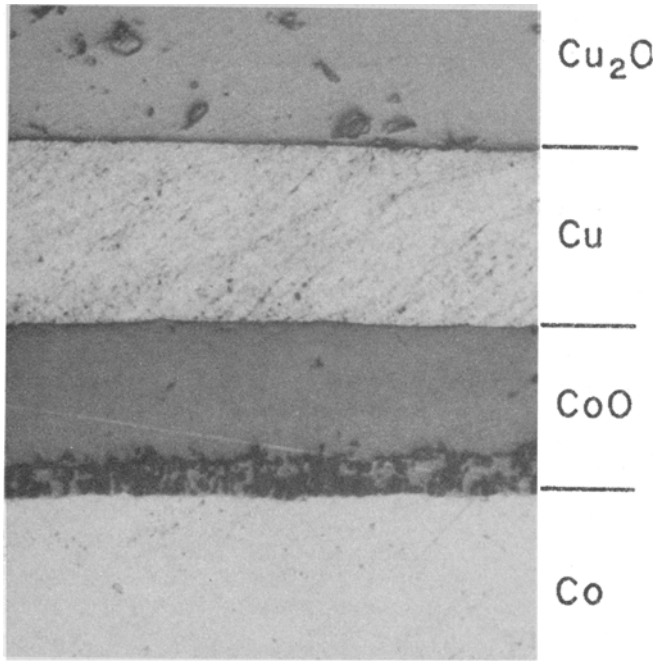

Fig. 5—Layered product morphology for the Co/Cu_2O displacement reaction after 25 h at 1000°C. Magnification 500 times.

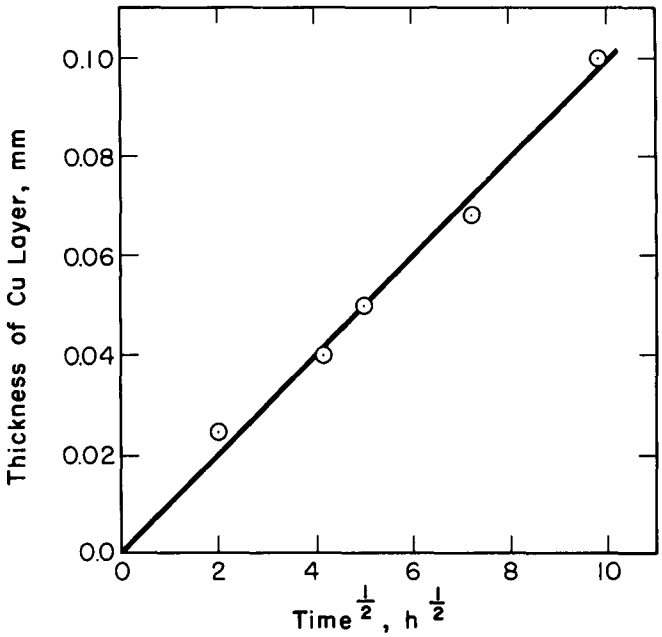

Fig. 6—Time dependence of the thickness of the product copper layer in the layered morphology for the Co/Cu_2O displacement reaction at 1000°C.

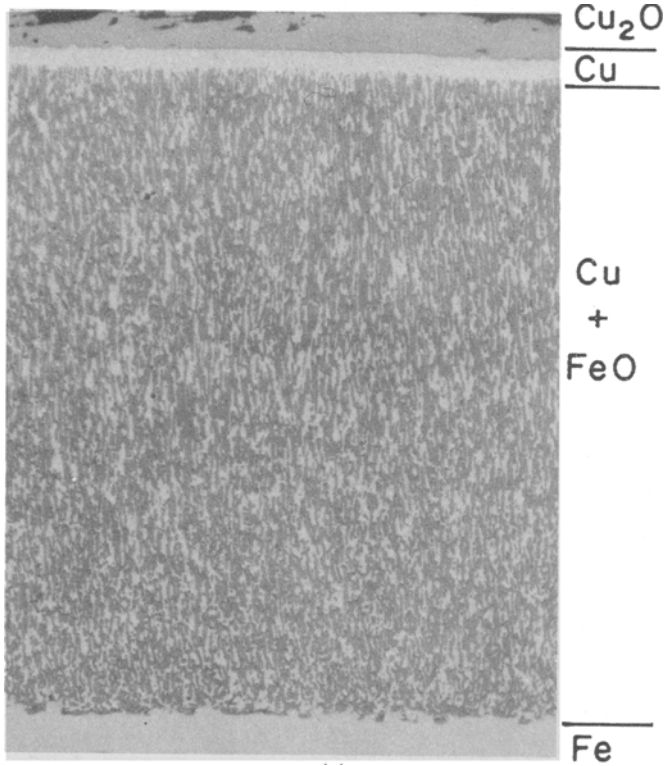

(*a*)

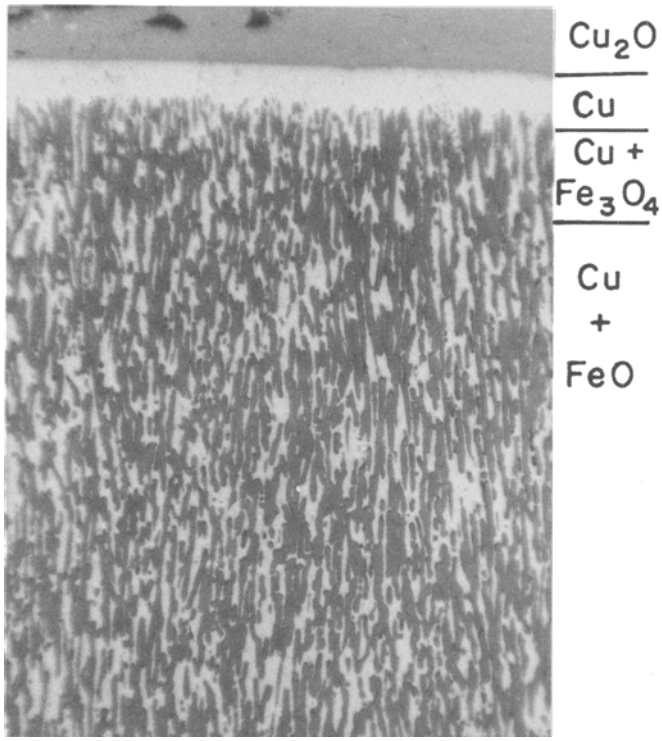

(*b*)

Fig. 7—Aggregate product morphology for the Fe/Cu_2O displacement reaction after one hour at 1000°C. (*a*) Magnification 200 times, (*b*) Magnification 400 times.

dopant ions, and therefore to less uncertainty in $D^*_{Co}(CoO)$. In addition, the CoO product was mostly compact. In contradiction to a previous study[1] of the Co/Cu_2O reaction at 800°C, the Co/Cu_2O reaction results in an ideal layered product morphology.

Fe/Cu_2O Reaction: The product zone of the Fe/Cu_2O displacement reaction at 1000°C consists of copper and iron oxide in an aggregate arrangement. Photomicrographs of the reaction products are shown in Fig. 7. The observed product morphology differs from the schematic model of Wagner, which is shown in Fig. 1(*b*), because a thin layer of copper separates the Cu_2O from the lamellar copper and iron oxide in the two-phase product zone. This is the first report of

this modified aggregate product morphology.

The iron oxide lamellae of the two-phase zone grow at their tips into the thin copper layer. As shown in the succeeding paper, the oxide lamellae consist primarily of wustite with a small amount of magnetite at the growth tips. The presence of the magnetite affects the details of the reaction mechanism, but it has only a small effect on the net rate of growth of the oxide lamellae. Because there is negligible diffusion of oxygen anions in FeO, growth of the iron oxide lamellae must occur by the diffusion of iron cations from the reactant iron through a continuous iron oxide phase to to the growth tips. Oxygen atoms, which are produced by the dissociation of Cu_2O at the Cu/Cu_2O interface, diffuse through the thin copper layer to the growing iron oxide lamellae.

As shown in Fig. 7, the copper in the two product zones is continuous. In order to examine the morphology of the oxide lamellae in greater detail, transverse and longitudinal sections of several reaction couples were examined with a scanning electron microscope.

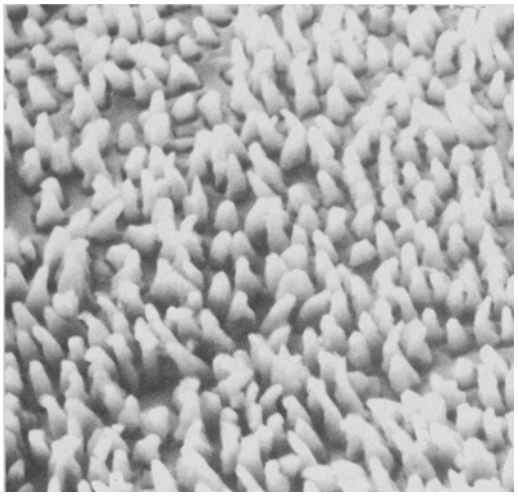

(*a*)

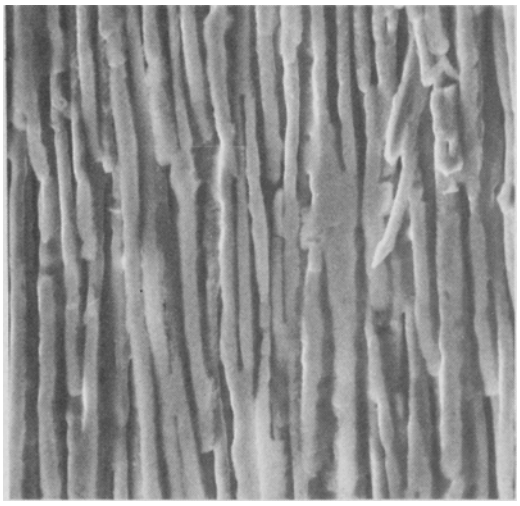

(*b*)

Fig. 8—Scanning electron micrographs of the product iron oxide lamallae after selective dissolution of the product copper for the Fe/Cu_2O displacement reaction at 1000°C. (*a*) Oxide growth tips, magnification 2000 times, (*b*) Oxide lamallae in the middle of the two-phase product zone, magnification 1000 times.

A transverse section was obtained by grinding away the Cu_2O which remained after the reaction until the product copper layer was exposed. The copper layer was then selectively dissolved by a solution of ammonium hydroxide and hydrogen peroxide until the growth tips of the product oxide were exposed, Fig. 8(*a*). A longitudinal section with the product copper selectively dissolved is shown in Fig. 8(*b*).

Fig. 8(*b*) shows that growth defects, such as branches and terminations, occur in the oxide lamellae. The apparent discrepancy between the sizes of the oxide lamellae shown in Figs. 7(*b*) and 8(*b*) must be explained by the partial dissolution of the oxide by the etchant. As required by the growth mechanism, the oxide phase is continuous across the two-phase product zone. The growth mechanisms of the copper and iron oxide products are discussed in more detail in the succeeding paper.

Plots of the thicknesses of the thin copper-layer and of the two-phase copper + iron oxide zone vs the square root of the reaction time are shown in Fig. 9; both of the zones grow according to parabolic kinetics. The

Table I. Predicted and Observed Morphologies and Rate Constants for Displacement Reactions at 1000°C

Reactive Couple	Calc. for Presupposed Layered Morphology, Equiv/cm-s		Morphology		k_p', cm²/s	
	k_r, Oxide	k_r, Metal	Pred.	Obs.	Calc.	Expt.
Ni/Cu_2O	1.4×10^{-13}	1.4×10^{-9}	layered	layered	1.3×10^{-12}	1.7×10^{-11}
Co/Cu_2O	5.3×10^{-12}	1.4×10^{-9}	layered	layered	4.7×10^{-11}	1.4×10^{-10}
Fe/Cu_2O	3.7×10^{-8}	1.4×10^{-9}	aggregate	aggregate	–	2.8×10^{-7} for Cu + FeO
					–	2.8×10^{-10} for Cu
						2.1×10^{-8}
Fe/NiO	3.7×10^{-8}	6.1×10^{-12}	aggregate	aggregate	–	NiO single crystal 9.1×10^{-8}
					–	NiO powder compact

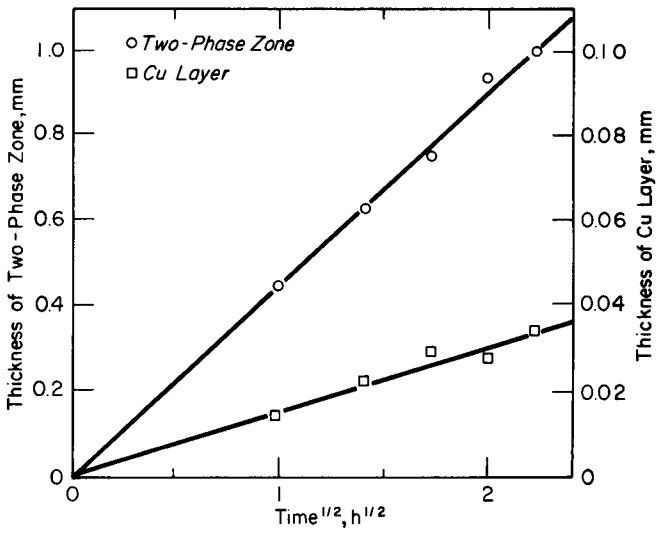

Fig. 9—Time dependence of the thickness of the copper layer and of the copper + iron oxide zone in the aggregate morphology for the Fe/Cu_2O displacement reaction at 1000°C.

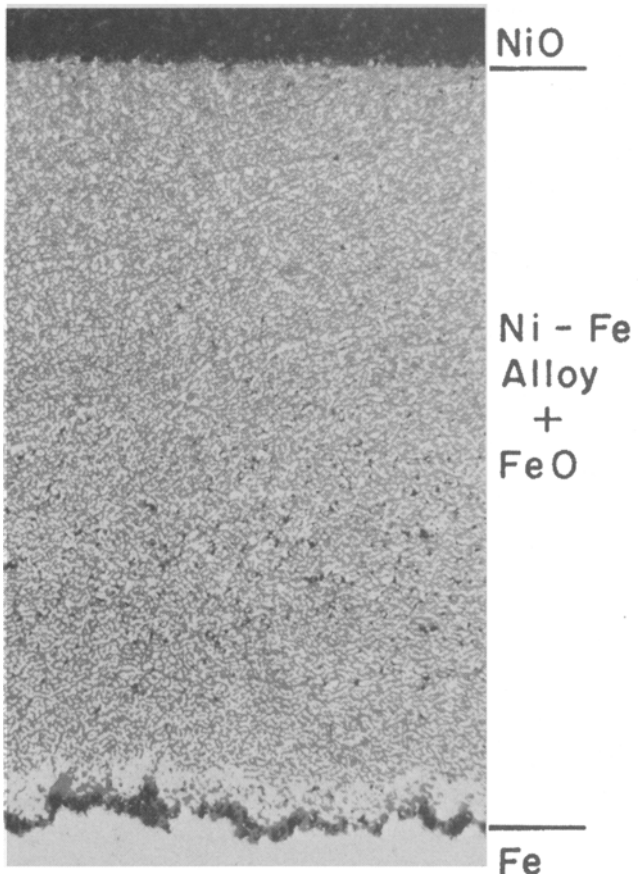

(*a*)

Fig. 10—Aggregate product morphology for the Fe/NiO (powder compact) displacement reaction after 9 h at 1000°C. (*a*) Magnification 125 times, (*b*) Magnification 700 times.

parabolic rate constants obtained from Fig. 9 are given in Table I.

Fe/NiO Reaction: The aggregate product morphology which results from the reaction of iron and a powder compact of NiO at 1000°C is shown in Figs. 10(*a*) and 10(*b*). The aggregate morphology was predicted from the calculated rate constants. In contrast to the arrangement of the product phases of the Fe/Cu_2O reaction, the Fe/NiO reaction results in a conglomerate of the product phases. Furthermore, a thin layer of product nickel is not formed between the NiO and the two-phase product zone.

The FeO phase of Fig. 10(*b*) is obviously continuous as is required for the transport of iron cations during the progress of the reaction. The nickel product phase of Fig. 10(*b*) is not obviously continuous, nor would that condition seem to be required by the growth mechanism because repeated nucleation and growth of nickel at the growth interface could be possible.

To examine more carefully the morphology of the nickel product phase in the two-phase field, the FeO phase was selectively dissolved by a solution of 25 pct concentrated HCl in ethyl alcohol. The remaining nickel phase was examined with a scanning electron microscope. As shown in Fig. 11, the nickel phase is completely continuous (as was the copper phase in the Cu + FeO product zone), and thus, the Ni + FeO product zone consists of two completely interwoven and continuous phases.

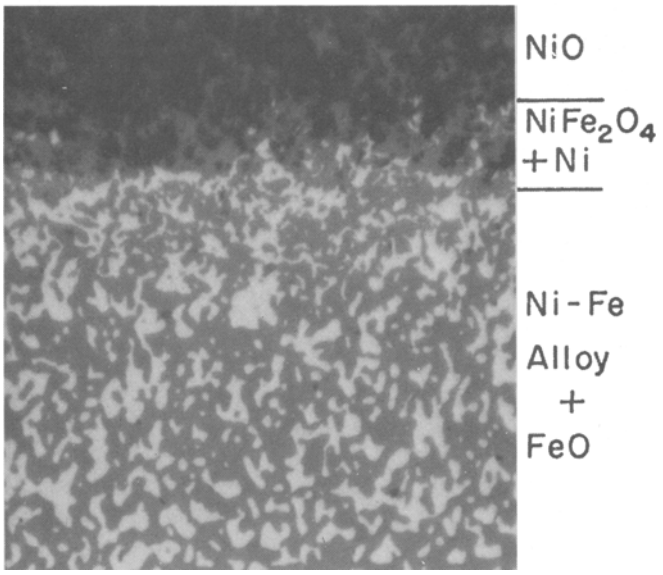

(*b*)

Fig. 10—Continued.

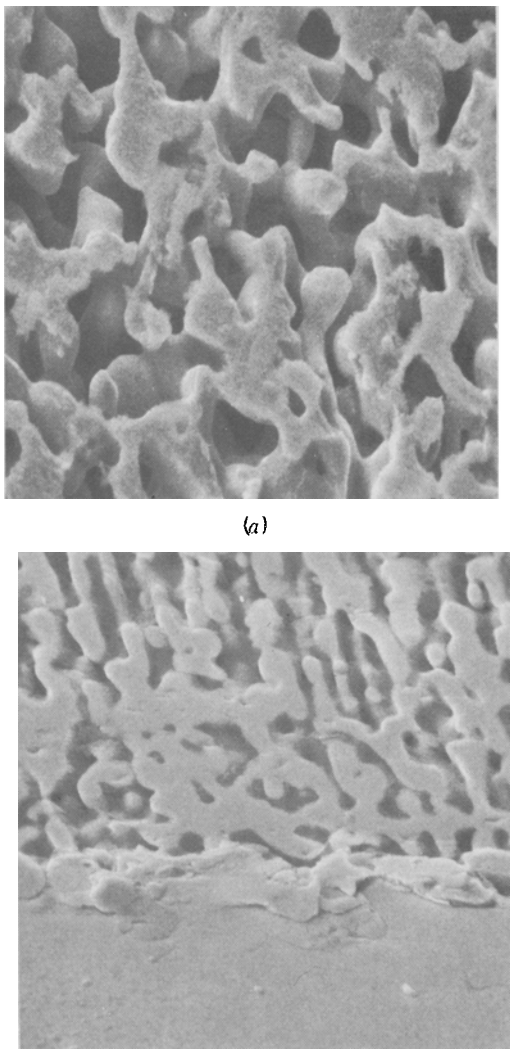

(*a*)

(*b*)

Fig. 11—Scanning electron micrographs of the product nickel after selective dissolution of the product FeO for the Fe/NiO (powder compact) displacement reaction at 1000°C. (*a*) Middle of the two-phase product zone, (*b*) iron/product zone interface. Magnification 2000 times.

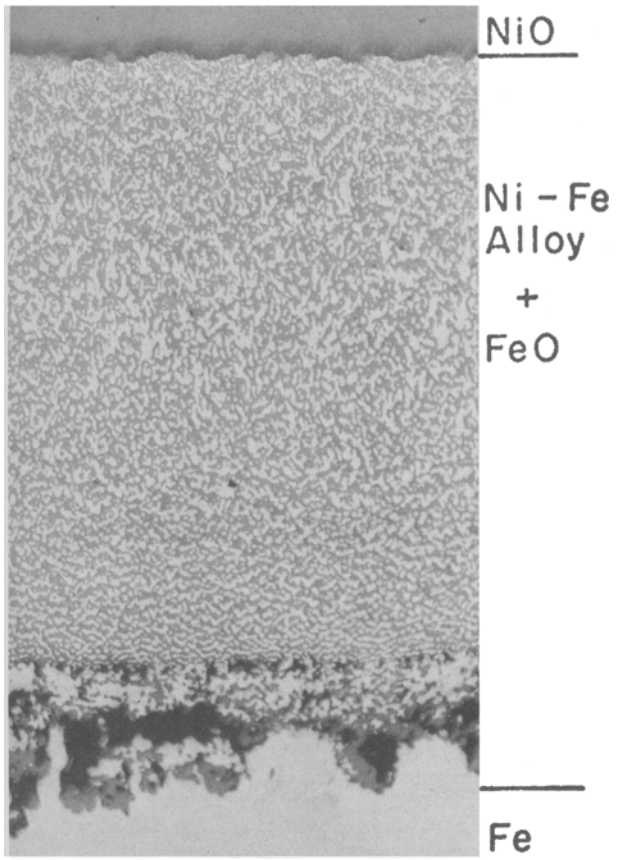

(*a*)

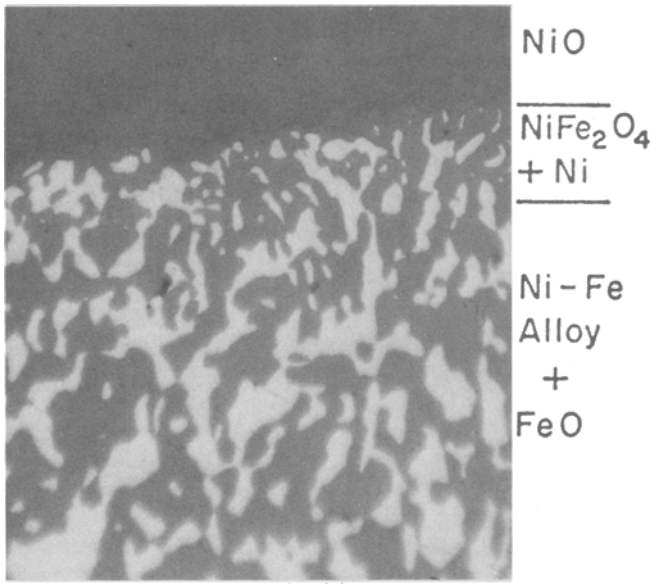

(*b*)

Fig. 12—Aggregate product morphology for the Fe/NiO (single crystal) displacement reaction after 64 h at 1000°C. (*a*) Magnification 95 times, (*b*) Magnification 700 times.

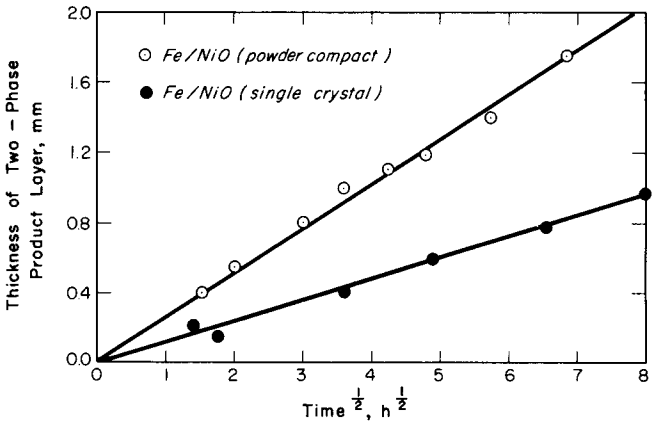

Fig. 13—Time dependence of the thicknesses of the aggregate product zones of the Fe/NiO (powder compact) and Fe/NiO (single crystal) displacement reactions at 1000°C.

This type of product arrangement; *i.e.*, the *interwoven*-aggregate arrangement, is a subgroup of the aggregate morphological class. The arrangement of the product phases of the Fe/Cu_2O reaction is the other subgroup; *i.e.*, the *lamellar*-aggregate arrangement. The reasons for the selection of a given subgroup by a reaction couple which should have the aggregate arrangement of product phases is a topic receiving further attention in our current research.

A scanning electron micrograph of the interface between the reactant iron and the Ni + FeO product zone after selective dissolution of the FeO is shown in Fig. 11(*b*). Normally, in the oxidation of iron to form FeO, a condensation of vacancies at the metal-scale interface leads to significant porosity, the ultimate loss of adherence, and a deviation from parabolic kinetics. While some disarrangement in the iron at the interface in Fig. 11(*b*) is present, gross porosity was not formed.

As expected from the isothermal section of the ternary Fe-Ni-O phase diagram at 1000°C,[20] the product zone of the Fe/NiO reaction does not consist simply of FeO and nickel. In particular, a band of nickel ferrite has been detected at the NiO/product interface by selective etching[20] and polarized light microscopy. The thickness of this band is small relative to the thickness of the entire product zone, and thus, its presence should have a negligible effect on the net reaction rate. The metallic phase which exists within the nickel ferrite band is presumably a nickel-rich alloy.

When single crystals of NiO instead of NiO powder compacts are used for the Fe/NiO reaction, similar product microstructures are obtained, as shown in Fig. 12. The product phases are also continuous and interwoven for this case, and nickel ferrite was again detected at the NiO/product interface by selective etching.

The main differences in the product morphologies which result when powder compacts or single crystals of NiO are used are the degree of fineness of the microstructure and the morphology at the NiO/product interface, as can be seen by comparing Figs. 10(*a*) and 10(*b*) with Figs. 12(*a*) and 12(*b*). This variation in product morphology is attributed to a difference in the reaction mechanism at the NiO/product interface, which results from the dissimilarity in the structure of the reactant NiO.

When sintered-powder compacts of NiO are employed the product nickel could form in voids which are present in the NiO. In this case, the fineness of the product morphology would be influenced by the pore size in the reactant NiO. Reactions using powder

compacts made from finer mesh NiO have indeed resulted in a finer product microstructure at the NiO/product interface. The NiO single crystals are not porous, and the nucleation and growth processes at the NiO/product interface are expected to be more complex for this case.

The thicknesses of the product zones for both the Fe/NiO (powder compact) and the Fe/NiO (single crystal) reactions are plotted as a function of the square root of the reaction time in Fig. 13. Parabolic growth kinetics is obeyed in each case. The difference in the reaction rates is also attributed to the difference in the growth processes at the NiO/product interfaces. Investigations are being conducted to ascertain the details of the mechanism of the Fe/NiO displacement reaction.

Engineering Implications

For a composite material, the interwoven product microstructure should be ideal both for the transfer of stresses and for resistance to crack propagation. In support of this statement, the product zones of Figs. 10 and 12 were not fractured by rapid cooling, in contrast to the layered product phases of Figs. 3 and 5. Thus, the interwoven-aggregate morphology should be the ideal arrangement of the product phases in the reaction zone between a compound fiber and a metallic matrix of a "reactive" or "incompatible" composite.

Consideration of the morphology selection criterion which was developed in this paper suggests that it might be possible to artificially control product morphologies, and thus the kinetics, for simple displacement reactions. An initial coating of sufficient thickness of the product metal between the reactants should cause the formation (at least initially) of the aggregate morphology regardless of the predictions based on equivalent thicknesses of the products. Likewise, an initial layer of the product oxide between the reactants should always effect the initiation of the layered arrangement. Because of potential applications to diffusion bonding and materials compatibility, this "control technique" may be of engineering importance.

The selective dissolution of either the metal or the oxide phase in the interwoven morphology should provide a means for the production of porous oxide or metal screens, respectively. Such porous materials enjoy a range of application, for example, as electrode materials in fuel cells and as catalysts for reactions between gases.

SUMMARY

A criterion for the prediction of the product morphologies for simple, solid-state displacement reactions has been developed. If the rate-controlling step in the growth of a presupposed layered arrangement of the product phases is diffusion in the oxide phase, then the layered morphology is stable. If the rate-controlling step is permeation of nonmetal through the metal phase, then the presupposed layered morphology is unstable and an aggregate arrangement of the product phases will result. Predictions based on this criterion have been supported by experimental observations for four reaction couples. The observed parabolic reaction kinetics for the reaction couples which exhibited the layered arrangement are comparable with the values calculated on the basis of available thermodynamic and kinetic data.

Two types of aggregate morphology, which have not been reported previously, have been identified; these are the lamellar-aggregate and the interwoven-aggregate morphologies.

ACKNOWLEDGMENTS

The authors wish to thank Dr. Robert Reeber for conducting preliminary experiments, R. Farrar for his use of the scanning electron microscope, and Professors Carl Wagner, John Hirth, and Gordon Powell for helpful discussions. This research was supported by contract AF33(615)-3948 of the Materials Laboratory at Wright-Patterson Air Force Base.

REFERENCES

1. C. Wagner: *Z. Anorg. Allgem. Chem.*, 1938, vol. 236, pp. 320-38.
2. C. Wagner: *J. Electrochem. Soc.*, 1956, vol. 103, pp. 571-80.
3. C. Wagner: *Z. Phys. Chem.*, 1969, vol. 64, pp. 49-53.
4. C. Wagner: *Z. Phys. Chem.*, 1936, vol. B32, pp. 447-62.
5. R. A. Rapp and D. A. Shores: in *Vol. IV, Techniques of Metals Research*, R. A. Rapp, ed., pp. 137 and 159, Wiley Publ., New York, 1970.
6. W. B. Crow: Ph.D. Thesis, Dept. Metall. Eng., Ohio State University, 1969.
7. R. Lindner and A. Akerstrom: *Disc. Faraday Soc.*, 1957, vol. 23, pp. 133-36.
8. J. J. Choi and W. J. Moore: *J. Phys. Chem.*, 1962, vol. 66, pp. 1308-11.
9. J. B. Price and J. B. Wagner: *Z. Phys. Chem., N. F.*, 1966, vol. 49, pp. 255-70.
10. J. B. Wagner: in *Mass Transport in Oxides Spec. Publ.* 296, J. B. Wachtman and A. D. Franklin, eds., pp. 65-77, 1968.
11. R. L. Pastorek and R. A. Rapp: *Trans. TMS-AIME*, 1969, vol. 245, pp. 1711-20.
12. P. Vallet and P. Raccah: *Mem. Sci. Rev. Met.*, 1965, vol. 62, pp. 1-29.
13. L. Himmel, R. F. Mehl, and C. E.Birchenall: *AIME Trans.*, 1953, vol. 197, pp. 827-43.
14. P. Hembree and J. B. Wagner: *Trans. TMS-AIME*, 1969, vol. 245, pp. 1547-52.
15. C. E. Birchenall: in *Heterogeneous Kinetics at Elevated Temperatures*, C. R. Belton and W. L. Worrell, eds., pp. 253-67, Plenum Press, N. Y., 1970.
16. C. B. Alcock and P. B. Brown: *J. Metal Sci.*, 1969, vol. 3, pp. 116-20.
17. W. B. Kerr and R. A. Rapp: The Ohio State University, Columbus, Ohio, unpublished research, 1972.
18. R. E. Carter and F. D. Richardson: *J. Metals*, 1954, vol. 6, pp. 1244-57.
19. J. G. Burt: *J. Electrochem. Soc.*, 1970, vol. 117, pp. 267-68.
20. A. D. Dalvi and W. W. Smeltzer: *J. Electrochem. Soc.*, 1970, vol. 117, pp. 1431-36.